# REPORT DOCUMENTATION PAGE

Form Approved
OMB No. 0704-0188

AD-A251 229



| 2. REPORT DATE | 3. REPORT TYPE AND DATES COVERED |
|---|---|
| 5/26/92 | Technical - 1 June, 1991 - 31 May, 1992 |

**4. TITLE AND SUBTITLE**
GaAs Deposition on the (100) and (110) Planes of Gold by Electrochemical Atomic Layer Epitaxy (ECALE). A LEED, AES and STM Study

**5. FUNDING NUMBERS**
G-N00014-19-J-1919

**6. AUTHOR(S)**
Ignacio Villegas and John L. Stickney

**7. PERFORMING ORGANIZATION NAME(S) AND ADDRESS(ES)**
University of Georgia
Department of Chemistry
Athens, GA 30602-2556

**8. PERFORMING ORGANIZATION REPORT NUMBER**
Technical Report #4

**9. SPONSORING/MONITORING AGENCY NAME(S) AND ADDRESS(ES)**
Office of Naval Research
Chemistry Division
Arlington, VA 22217-5000



**10. SPONSORING/MONITORING AGENCY REPORT NUMBER**

**11. SUPPLEMENTARY NOTES**

**12a. DISTRIBUTION/AVAILABILITY STATEMENT**
Approved for public release and sale; its distribution is unlimited

**12b. DISTRIBUTION CODE**

**13. ABSTRACT** *(Maximum 200 words)*

Preliminary studies on the deposition of GaAs by electrochemical atomic layer epitaxy (ECALE) were performed. ECALE is based on the alternated underpotential deposition (UPD) of atomic layers of different elements to form a compound. Oxidative UPD of As and reductive UPD of Ga on the low-index planes of gold were studied using Auger electron spectroscopy (AES), low energy electron diffraction (LEED), scanning tunneling microscopy (STM) and coulometry. AES and LEED were performed in an ultrahigh vacuum (UHV) surface analysis instrument interfaced to an electrochemical cell in an antechamber. This instrument configuration allowed the electrochemical treatment of the samples and their subsequent analysis in UHV without the need to transfer the samples through air. STM was performed under nitrogen at atmospheric pressure. AES and coulometry were used for surface composition analysis while LEED and STM provided structural information. The substrate was a gold single-crystal electrode with three oriented faces, each to a different low-index plane. Oxidative UPD of arsenic was observed only on the (100) and (110) faces. The resulting structures were a Au(100)(2X2)-As at 1/4 coverage and a Au(110)c(2X2)-As at 1/2 coverage.

| 14. SUBJECT TERMS | 15. NUMBER OF PAGES |
|---|---|
| GaAs, Electrodeposition, ALE, Gold Single Crystals | 27 |
| | 16. PRICE CODE |

| 17. SECURITY CLASSIFICATION OF REPORT | 18. SECURITY CLASSIFICATION OF THIS PAGE | 19. SECURITY CLASSIFICATION OF ABSTRACT | 20. LIMITATION OF ABSTRACT |
|---|---|---|---|
| Unclassified | Unclassified | Unclassified | UL |

OFFICE OF NAVAL RESEARCH

GRANT or CONTRACT N00014-91-J-1919

R&T Code 4133036

Technical Report No. 4

# GaAs Deposition on the (100) and (110) Planes of Gold by Electrochemical Atomic Layer Epitaxy (ECALE). A LEED, AES and STM Study.

by

Ignaico Villegas and John L. Stickney

Prepared for Publication

in the

Journal of Vacuum Science and Technology A

Department of Chemistry
University of Georgia
Athens, Georgia 30602

May 26, 1992





# GaAs Deposition on the (100) and (110) Planes of Gold by Electrochemical Atomic Layer Epitaxy (ECALE). A LEED, AES and STM Study.

Ignacio Villegas and John L. Stickney*

Department of Chemistry
University of Georgia
Athens, GA 30602

* To whom correspondence should be addressed.

## ABSTRACT

Preliminary studies on the deposition of GaAs by electrochemical atomic layer epitaxy (ECALE) were performed. ECALE is based on the alternated underpotential deposition (UPD) of atomic layers of different elements to form a compound. Oxidative UPD of As and reductive UPD of Ga on the low-index planes of gold were studied using Auger electron spectroscopy (AES), low energy electron diffraction (LEED), scanning tunneling microscopy (STM) and coulometry. AES and LEED were performed in an ultrahigh vacuum (UHV) surface analysis instrument interfaced to an electrochemical cell in an antechamber. This instrument configuration allowed the electrochemical treatment of the samples and their subsequent analysis in UHV without the need to transfer the samples through air. STM was performed under nitrogen at atmospheric pressure. AES and coulometry were used for surface composition analysis while LEED and STM provided structural information. The substrate was a gold single-crystal electrode with three oriented faces, each to a different low-index plane. Oxidative UPD of arsenic was observed only on the (100) and (110) faces. The resulting structures were a Au(100)(2×2)-As at 1/4 coverage and a Au(110)c(2×2)-As at 1/2 coverage. Reductive UPD of Ga was observed on all three faces, although it resulted in disordered layers of Ga oxide upon removal of the substrate from solution, due to partial oxidation of the Ga in contact with water in the absence of potential control. Stoichiometric coverages of Ga and As were obtained on the (100) and (110) surfaces when Ga was underpotentially deposited on the As covered surfaces (Au(100)(2×2)-As at 1/4 coverage and Au(110)c(2×2)-As at 1/2 coverage). Structures displaying (2X2) and c(2X2) LEED patterns were observed on the (100) and (110) faces, respectively.

## INTRODUCTION

The preparation of compound semiconductors, II-VI and III-V materials in particular, by electrochemical deposition has been the object of a number of studies during the last twenty years. The development of new, low temperature methods of deposition is an important area of research. Electrochemical deposition represents an alternate methodology to prepare compound semiconductors at room temperature, which could avoid interdiffusion problems associated with the high temperatures required in current deposition techniques [1].

Research in our laboratory is directed towards the development of a method to epitaxially electrodeposit compound semiconductors from aqueous solutions: electrochemical atomic layer epitaxy (ECALE) [2]. Previous attempts to electrodeposit compound semiconductors have resulted in polycrystalline deposits. An important example of previous deposition methodology was developed by Kroger *et al.* [3]. That method consists of the simultaneous codeposition of both component elements from oxidized species in a single solution. The deposition potential is chosen in order to optimize the stoichiometry of the deposits. Generally, the deposition potential is such that one of the elements is deposited at a rate controlled by mass transfer towards the electrode surface. The other element, present in excess, reacts with the previously deposited element to form the compound. The ECALE methodology is intended to address problems associated with nucleation and growth. ECALE is based on the alternated electrodeposition of atomic layers of the component elements from two different solutions. Underpotential deposition (UPD) is a surface-limited process where an atomic layer of one element is deposited on a substrate surface composed of a different element at a potential prior to that required for bulk deposition of the first element [4,5]. ECALE takes advantage of this surface-limited process to alternately deposit atomic layers of the desired elements, thus eliminating three-dimensional nucleation.

Previous studies in our laboratory have concentrated on the ECALE deposition of CdTe [2,6,7]. Preliminary studies involved the UPD of Cd and Te on different polycrystalline substrates (Au, Pt and Cu) using thin-layer electrochemical cells [7]. Au was selected as the most applicable substrate for subsequent studies of ECALE deposition due to its extended double-layer window which allows the study of UPD with minimum interference from substrate oxidation and hydrogen evolution processes. A fortuitous lattice mismatch of only 3.5 % exists between GaAs and twice the Au lattice constant. UPD of Cd and Te on the three low-index planes of gold was studied using AES and LEED [6,8]. The studies described in this manuscript are the continuation of a previous study on the ECALE deposition of GaAs on the three low-index planes of gold [9].

GaAs has been successfully electrodeposited from aqueous solutions [10,11] and from molten salt electrolytes [12,13]. The formation of GaAs was confirmed by X-ray and electron diffraction measurements, although the deposits obtained were polycrystalline in each case. The thermodynamic stability of GaAs in aqueous solutions has been addressed in a number of studies. The stability of materials in aqueous solutions are usually evaluated through potential versus pH plots (Pourbaix diagrams). In earlier studies, the stability of GaAs in aqueous solutions was questioned [10,14]. More accurate diagrams have been calculated [15] and a region of thermodynamic stability between pH 1.3 and pH 13.3 was determined. Our own studies, including calculations which take into consideration a number of concentrations of the different species in solution in contact with the GaAs, indicate the possibility of obtaining stable GaAs deposits in aqueous solutions as long as potential control is maintained.

The electrochemistry of As has been extensively studied and reported in the literature [16,17]. A mechanism has been proposed for the deposition of As on gold, involving three successive one electron transfers and passivation due to the formation of an amorphous layer of As [17]. The electrochemistry of Ga has been studied as well [18].

Preliminary studies of the ECALE deposition of GaAs were performed using a thin-layer electrochemical cell (TLE) with a polycrystalline gold electrode [9]. Potentials for Ga and As UPD on gold were evaluated. It was determined that Ga UPD occurs 50 mV prior to the hydrogen evolution reaction during the negative scan. Bulk Ga is deposited at potentials more negative than the potential for hydrogen evolution. Arsenic was shown to be reductively deposited from a $HAsO_2$ (pH 4) solution between -0.3 and -1.5 V in a three electron transfer according to the reaction

$$HAsO_2 + 3H^+ + 3e^- \rightarrow As + 2H_2O \qquad (1).$$

The onset potential for deposition depends on the pH of the solution, shifting towards more negative potentials as the pH increases. It was also found that As coverage reaches a maximum independent of the pH of the solution [9,16,17,19-23]. The potential at which the maximum coverage is reached also shifts towards more negative potentials as the pH of the solution increases. The decrease in As coverage at very negative potentials is due to the reaction

$$As + 3H^+ + 3e^- \rightarrow AsH_3 \qquad (2).$$

Formation of arsine from As reduction in aqueous solutions has been reported in the literature [24]. The minimum As coverage at negative potentials is about 0.4 As atoms per surface Au atom and is independent of pH for solution pHs higher than 3. For pHs lower than 3, arsine formation is inhibited by depolarization of the electrode potential due to extensive hydrogen evolution. This results in the higher As coverage at potentials below -1.0 V, as the electrode never really attains those highly negative potentials. There are two ways of looking at these results. Deposited arsenic is reduced to arsine at very negative potentials according to reaction 2, leaving behind an atomic layer of As, stabilized by bonding with Au surface atoms. Alternatively, $HAsO_2$ can be considered to convert quantitatively to arsine according to the reaction

$$HAsO_2 + 6H^+ + 6e^- \rightarrow AsH_3 + 2H_2O \qquad (3)$$

and an atomic layer of As is deposited by oxidative UPD from arsine.

## EXPERIMENTAL

A combination of ultrahigh vacuum (UHV) and ambient pressure surface characterization techniques were used in these studies. The UHV surface analysis instrument included a hemispherical electron analyzer and electron gun for Auger electron spectroscopy (AES) and a set of low energy electron diffraction (LEED) optics. Electrochemical experiments were performed in an UHV antechamber interfaced to the main analysis chamber. This configuration enables the electrochemical treatment of the samples in an argon atmosphere at ambient pressure and their subsequent analysis in UHV without the need to transport the samples through air. This instrument has been described in detail in previous publications [9,25]. Surface characterization in UHV included AES and LEED, which provided information about the elemental and structural composition of the surfaces, respectively. AES parameters were as follows: 1 $mm^2$ beam size, 10 $\mu A$ beam current at 3000 V, 5 minute 100 - 600 eV and 3 min 1000 - 1300 eV scans.

The gold substrate was a single crystal which had been oriented, using Laué X-ray diffraction, cut and mechanically polished to expose the three low-index planes on three different faces. Electrical connection was made through a gold wire, avoiding the use of other materials which could interfere in the electrochemistry. Surface preparation prior to electrochemical experiments consisted of ion bombardment with 300 V $Ar^+$ ions for one hour and subsequent annealing at 650 °C. The cleanliness and order of the surfaces was monitored using AES and LEED.

A NanoScope II (Digital Instruments) was used in scanning tunneling microscopy (STM) experiments. Electrochemistry and subsequent STM characterization were performed inside a glove box in a nitrogen atmosphere at ambient pressure. STM tips were prepared by electrochemically etching a tungsten wire in 1.0 M NaOH. The substrate used for STM experiments was a gold single crystal, oriented, cut and polished to expose the (100) plane on all six sides of a rectangular box.

All solutions used in these studies were prepared with research grade chemicals and pyrolytically triply-distilled water [26]. Potentials are reported versus a Ag/AgCl, 1.0 M NaCl reference electrode.

## RESULTS AND DISCUSSION

No signals other than those assignable to Au were observed in the Auger spectra of the three ion bombarded and annealed surfaces of the gold tri-crystal (Figure 1a). Reconstructions were evident in the LEED patterns for the three surfaces [27]. The voltammogram obtained with the clean Au tri-crystal in 1.0 mM $HAsO_2$/1.0 mM $H_2SO_4$ (pH 3.2) is shown in Figure 2a. This voltammogram is analogous to those reported in the literature [9,17]. Oxidative UPD of As on the low-index planes of gold was evaluated as follows. The tri-crystal was immersed in a 1.0 mM $HAsO_2$/1.0 mM $H_2SO_4$ (pH 3.2) solution at a series of potentials between -1.0 V and -1.6 V for 30 seconds. The electrode was subsequently emersed (removed) from the $HAsO_2$ solution and rinsed three times with 10.0 mM $H_2SO_4$ (pH 1.9) at controlled potential, with the final rinse held for one minute. Characterization of the surfaces was performed by AES and LEED. Similar procedures were employed using a 10.0 mM $Cs_2SO_4$ solution, containing a 1.0 mM acetate buffer (pH 4.7) instead of the 10.0 mM $H_2SO_4$. Emersion from this solution resulted in some excess $Cs_2SO_4$ crystallizing on the surface, which interfered with the As quantitation. For this reason, a final rinse with dilute $H_2SO_4$ was added after emersion from $Cs_2SO_4$. In each case the initial deposition potential was maintained for all stages where the electrode was in solution. The total As coverage at each potential was determined by subsequent stripping in 10.0 mM $H_2SO_4$, after the surface characterization had been completed. Coulometric measurements determine the total amount of As deposited on all three faces. Total As coverages as a function of the deposition potential and the pH of the initial reduction solution are presented in Figure 3. The coverage of As

plateaus at 0.4 for potentials between -1.2 V and -1.5 V in the pH 4.7 solution. Arsine formation is inhibited by depolarization of the electrode, due to hydrogen evolution in the pH 1.9 solution, resulting in higher As coverages at very negative potentials. These results are analogous to those obtained in studies of oxidative As UPD using TLEs with polycrystalline Au electrodes [9]. Transitions assignable to Au and As were the only observable features in the Auger spectra obtained for the (100) and (110) surfaces at deposition potentials in the plateau region (pH 4.7 solution). A representative spectrum is shown in Figure 1b. Auger spectra for the (111) surface displayed only Au transitions, no detectable As signal. For potentials in the plateau region, (2X2) (Figure 4a) and c(2X2) (Figure 5a) LEED patterns were obtained for the (100) and (110) surfaces, respectively. Proposed low-coverage structures are shown in Figures 4b and 5b: a Au(100)(2X2)-As at 1/4 coverage and a Au(110)c(2X2)-As at 1/2 coverage. Higher As coverages resulted only in diffuse LEED patterns for the three low-index planes.

An atomic layer of As was deposited on a six-sided Au(100) crystal (described in the experimental section) by oxidative UPD at -1.3 V at pH 4 according to the procedure described above. The crystal was positioned in the microscope such that rows of atoms in the (100) lattice, the [110] direction, would appear at 45° ± 5° angles with respect to the horizontal of the instrument's screen. Figure 6 is a picture of the instrument's screen showing a Au(100)(2×2)-As structure. The As-As distance corresponds, within experimental error, to twice the Au-Au distance in the (100) lattice. A 45° angle (± 5°) with respect to the horizontal of the screen is also consistent with a (2X2) structure. A similar structure has been observed for a Au(100)(2×2)-Te structure at 1/4 coverage, reported in this same issue [28].

Figure 2d shows a voltammogram obtained with the Au tri-crystal in a 0.5 mM $Ga_2(SO_4)_3$ (pH 2.7) solution. In previous studies, it had been determined that the peak at -0.5 V corresponds to the reductive UPD of Ga, while bulk deposition was obscured by hydrogen evolution. The peaks observed during the subsequent positive scan correspond to bulk Ga stripping at -0.6 V and Ga UPD stripping at -0.4 V. Similar Auger spectra were obtained for the three low-index planes emersed from solution just

before the Ga UPD stripping peak during the positive scan. Transitions corresponding to Au, Ga and O were evident in the spectra (Figure 1c). Completely diffuse LEED patterns were observed for each of the three faces. The presence of oxygen on the surfaces is attributed to partial oxidation of the deposited Ga after emersion and loss of potential control. This is understandable as the electrode remained in contact with a thin-layer of solution upon emersion (the emersion layer). Partial oxidation of the Ga in contact with an aqueous solution, without potential control, is consistent with the thermodynamic stability of Ga(0) in the presence of $H_2O$ [29]. Integration of the UPD Ga stripping peak resulted in an overall Ga coverage of 0.2 - 0.3, as long as the electrode was not emersed prior to stripping.

In order to investigate the ECALE deposition of GaAs, the alternated deposition of Ga and As was also investigated. Arsenic was first deposited from a 1.0 mM $HAsO_2$/1.0 mM $H_2SO_4$ (pH 3.2) solution and subsequently reduced in a buffered 10.0 mM $Cs_2SO_4$ (pH 4.7) solution at -1.25 V, according to the procedure described previously. The next step consisted of a series of experiments in which the As-covered surfaces were immersed in a 0.5 mM $Ga_2(SO_4)_3$ (pH 2.7) solution at various potentials between -0.96 and -0.40 V. For Ga deposition potentials between -0.71 and -0.56 V, stoichiometric amounts of Ga, relative to the previously deposited As, were deposited on the (100) and (110) surfaces, as shown by AES (Figure 1d). Bulk Ga deposition occurred at potentials more negative than -0.71 V, while no Ga was deposited at potentials more positive than -0.56 V. Auger transitions for Au, Ga, As and O are evident in Figure 1d. The presence of oxygen on the surface is probably due to partial oxidation of the GaAs upon emersion of the electrode from solution. GaAs in contact with water at open circuit can oxidize to form $Ga_2O_3$ and As [9].

Stoichiometric coverages of Ga and As resulted in (2X2) (Figure 7a) and c(2X2) (Figure 8a) LEED patterns on the Au(100) and Au(110) surfaces, respectively. Partial oxidation of the Ga, as indicated by AES, accounts for the extra diffuseness observed in the LEED patterns displayed in Figures

7a and 8a when compared with the LEED patterns obtained for the As-covered surfaces (Figures 4a and 5a). Partial oxidation of Ga deposited on arsenic-free Au surfaces resulted in completely diffuse LEED patterns. Enhanced stability due to compound formation when Ga is deposited on As-covered Au surfaces is probably responsible for the increased order observed in Figures 7a and 8a compared to the studies made sans As. Proposed structures corresponding to monolayers of GaAs on the Au(100) and the Au(110) surfaces are shown in Figures 7b and 8b. These structures were drawn using the atomic radii of Ga and As [30]. The proposed Au(100)(2X2)-GaAs structure involves stoichiometric coverages of Ga and As, and the formation of As dimers on the surface. Dimerization has been reported in the literature, supported by LEED and STM results [31-35]. Stoichiometric coverages of Ga and As on the Au(100) surfaces without dimerization of As would probably result in a c(2X2) LEED pattern, but no signs of this pattern were observed in our studies. The proposed Au(110)c(2X2)-GaAs structure, shown in Figure 8b, also requires stoichiometric coverages of Ga and As. No dimers are proposed in this case. STM results on GaAs(110) also indicate no dimer formation [36-38]. The (110) surface is more open, permitting both Ga and As bonding to Au surface atoms. The proposed structures resemble truncation of a GaAs crystal through the (100) and (110) planes, respectively, due to the decent match between the GaAs lattice constant (5.65 Å) and twice the Au lattice constant (5.84 Å). Problems with the lattice match and the critical thickness will occur as the film thickness is increased, as is the topic of further studies.

Potential versus pH plots have been calculated in order to evaluate the stability of GaAs under the conditions to be used for ECALE [9]. According to those plots, a spontaneous reaction may occur between $H^+$ in solution and GaAs at open circuit. Our calculations showed that GaAs can exist in aqueous solutions as long as the potential is kept within the region of stability. For that reason, successful formation of thicker films of GaAs by the ECALE method will be achieved only if potential control is maintained at all times. The experimental procedure described above involves emersion of the substrate and loss of potential control after each deposition and rinsing step, resulting in partial oxidation

of Ga after it has been deposited. Partial oxidation of the Ga upon emersion of the substrate accounts for the oxygen present in the Auger spectra of the GaAs-covered surfaces. A thin-layer flow cell is being developed in our laboratory, which will enable the exchange of solutions for successive UPD of atomic layers of Ga and As without emersion and loss of potential control.

In conclusion, oxidative UPD of As resulted in ordered layers on the (100) and (110) surfaces of Au. A Au(100)(2X2)-As at 1/4 coverage (Figures 4b and 6) and a Au(110)c(2X2)-As at 1/2 coverage (Figure 5b) are proposed. Reductive UPD of Ga was achieved on the three low-index planes of Au, but resulted a layer of disordered Ga oxide on the three low-index planes of gold after emersion. Successive UPD of atomic layers of As and Ga resulted in ordered structures on the Au(100) and Au(110) surfaces: a Au(100)(2X2)-GaAs (Figure 7b) and a Au(110)c(2X2)-GaAs (Figure 8b). Proposed structures consist of stoichiometric coverages of Ga and As, and As dimers are proposed to explain the (2X2) LEED pattern observed on the (100) surface [31-35].

## ACKNOWLEDGEMENTS

Acknowledgment is made to the Donors of The Petroleum Research Fund, administered by the American Chemical Society, for partial support of this research. Acknowledgment is also given to the National Science Foundation, for partial support of this work under grant Nº DMR-9017431. This work is partially sponsored by the Department of the Navy, office of the Chief of Naval Research, under grant Nº N00014-91-J-1919. I.V. would like to thank INTEVEP S.A. (Caracas, Venezuela) for financial support.

## REFERENCES


1. H. Watanabe, T. Mizutani and A. Usui, in "*Very High Speed Integrated Circuits: Heterostructures*", T. Ikoma, Editor, Semiconductors and Semimetals, Vol. 30, Academic Press, Inc., New York, 1990, pg. 1.

2. B.W. Gregory and J.L. Stickney, *J. Electroanal. Chem.* **300**, 543 (1991).

3. F.A. Kröger, *J. Electrochem. Soc.* **125**, 2028 (1978).

4. D.M. Kolb, in "*Advances in Electrochemistry and Electrochemical Engineering*," H. Gerischer and C.W. Tobias, Editors, Vol. 11, John Wiley, New York (1978).

5. K. Juttner and W.J. Lorenz, *Z. Phys. Chem. N.F.* **122**, 163 (1980).

6. B.W. Gregory, D.W. Suggs and J.L. Stickney, *J. Electrochem. Soc.* **138**, 1279 (1991).

7. B.W. Gregory, M.L. Norton and J.L. Stickney, *J. Electroanal. Chem.* **293**, 85 (1990).

8. D.W. Suggs and J.L. Stickney, *J. Phys. Chem.* (in press).

9. I. Villegas and J.L. Stickney, *J. Electrochem. Soc.* (submitted for publication)

10. S. Chandra and N. Khare, *Semicond. Sci. Technol.* **2**, 214 (1987).

11. S. Chandra and N. Khare, *Semicond. Sci. Technol.* **2**, 220 (1987).

12. R.C. De Mattei, D. Elwell and R.S. Feigelson, *J. Cryst. Growth* **43**, 643 (1978).

13. I. G. Dioum, J. Vedel and B. Tremillon, *J. Electroanal. Chem.* **139**, 329 (1982).

14. S.-M. Park and M.E. Barber, *J. Electroanal. Chem.* **99**, 67 (1979).

15. G.G. Perrault, *J. Electrochem. Soc.* **136**, 2845 (1989).

16. A.P. Tomilov and N.E. Chomutov, in "*Encyclopedia of Electrochemistry of the Elements*," A.J. Bard, Editor, Vol. II, Chap. 2, Marcel Dekker, inc., New York (1974).

17. T.E. Dinan, W.-F Jou and H.Y. Cheh, *J. Electrochem. Soc.* **136**, 3284 (1989).

18. T.I. Popova and I.A. Bagotskaya, in "*Encyclopedia of Electrochemistry of the Elements*," A.J. Bard, Editor, Vol. VIII, Chap. 3, Marcel Dekker, inc., New York (1978).

19. W. Stillwell and L.F. Audrieth, *J. Am. Chem. Soc.* **54**, 472 (1932).

20. G. Wranglén, *J. Electrochem. Soc.* **108**, 1069 (1961).

21. R. Piontelli and G. Poli, *J. Electrochem. Soc.* **109**, 551 (1962).

22. G. Wranglén, *J. Electrochem. Soc.* **109**, 552 (1962).

23. I.A. Menzies and L.W. Owen, *Electrochim. Acta* **11**, 251 (1966).

24. H.W. Salzberg and B. Goldschmidt, *J. Electrochem. Soc.* **107**, 348 (1960).

25. J.L. Stickney, B.W. Gregory and C.B. Ehlers, in "*Electrichemical Surface Science*", edited by M.P. Soriaga (ACS Symposium Series 378, American Chemical Society, Washington D.C., (1988), p. 99.

26. B.E. Conway, H. Angerstein-Kozlowska, W.G.A. Sharp and E.E. Criddle, *Anal. Chem.* **45**, 1331 (1973).

27. D.M. Kolb and J. Schneider, *Electrochim. Acta* **31**, 929 (1986).

28. D.W. Suggs, I. Villegas, B.W. Gregory and J.L. Stickney, *J. Vac. Sci. Tech.* (this issue).

29. M.J.N. Pourbaix, "*Atlas of the Electrochemical Equilibria in Aqueous Solutions*," Pergamon Press, New York (1966).

30. Table of Periodic Properties of the Elements, Sargent-Welch Scientific Company, Chicago. 1968.

31. P.K. Larsen and G. Meyer-Ehmsen, *Surf. Sci.* **240**, 168 (1990).

32. H.H. Farrell, M.C. Tamargo and J.L. de Miguel, *Appl. Phys. Lett.* **58**, 355 (1991).

33. C. Deparis and J. Massies, *J. Cryst. Growth* **108**, 157 (1991).

34. M.D. Pashley, K.W. Haberern, W. Friday, J.M. Woodall and P.D. Kirchner, *Phys. Rev. Lett.* **60**, 2176 (1988).

35. B.K. Biegelsen, L.-E. Swartz and R.D. Brigans, *J. Vac. Sci. Technol.* **A8**, 280 (1990).

36. R.M. Feenstra and A.P. Fein, *Phys. Rev. B* **32**, 1394 (1985).

37. J.A. Stroscio, R.M. Feenstra, D.M. Newns and A.P. Fein, *J. Vac. Sci. Technol.* **A6**, 499 (1988).

38. J. Tersoff, R.M. Feenstra, J.A. Stroscio and P. Fein, *J. Vac. Sci. Technol.* **A6**, 497 (1988).

## FIGURES

Figure 1. Auger spectra:
a) Ion bombarded and annealed Au(100).
b) As oxidative UPD on Au(100).
c) Ga reductive UPD on Au(100).
d) Stoichiometric coverage of Ga and As on Au(100).

Figure 2. Cyclic voltammograms of the Au tri-crystal:
a) clean in 1.0 mM $HAsO_2$, 1.0 mM $H_2SO_4$ (pH = 3.2) (scan rate = 5 mV/sec).
b) clean in 0.5 mM $Ga_2(SO_4)_3$ (pH = 2.7) (scan rate = 5 mV/sec).

Figure 3. Total As coverage versus deposition potential and pH on the Au tri-crystal.

Figure 4. (a) Picture of the (2X2) LEED pattern obtained at 1/4 As coverage on Au(100) (beam energy = 38eV).
(b) proposed structure for As UPD (1/4 coverage) on Au(100).

Figure 5. (a) Picture of the c(2X2) LEED pattern obtained at 1/2 As coverage on Au(110) (beam energy = 39 eV).
(b) proposed structure for As UPD (1/2 coverage) on Au(110).

Figure 6. STM image of the Au(100)(2×2)-As structure.

Figure 7. (a) Picture of the (2X2) LEED pattern obtained at stoichiometric coverages of Ga and As on Au(100) (beam energy = 37 eV).
(b) proposed structure for stoichiometric coverages of Ga and As on Au(100). (As: dark gray, Ga: light gray, Au: white)

Figure 8. (a) Picture of the c(2X2) LEED pattern obtained for stoichiometric coverages of Ga and As on Au(110) (beam energy = 37 eV).
(b) proposed structure for stoichiometric coverages of Ga and As on Au(110). (As: dark gray, Ga: light gray, Au: white)

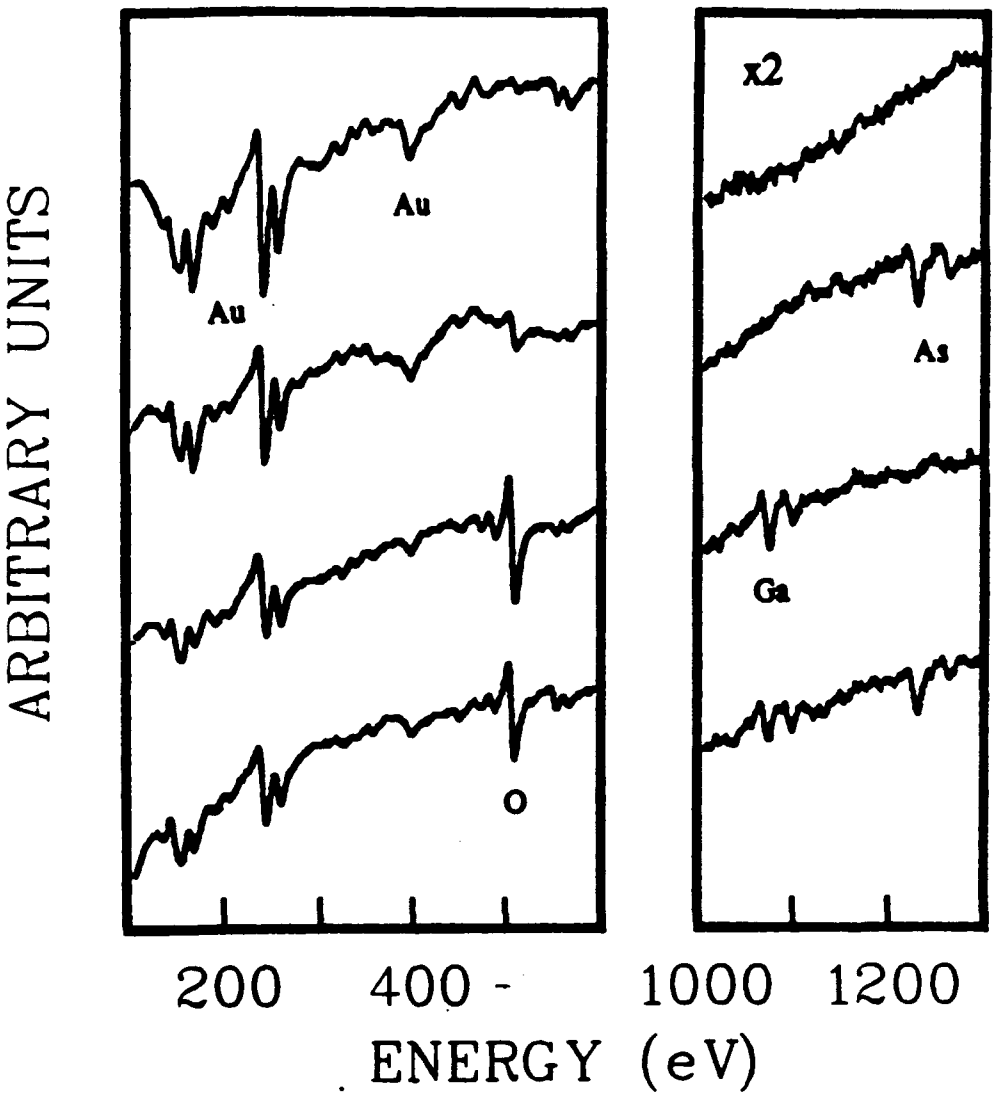


Figure 1. I. Villegas and J.L. Stickney. GaAs Deposition ...

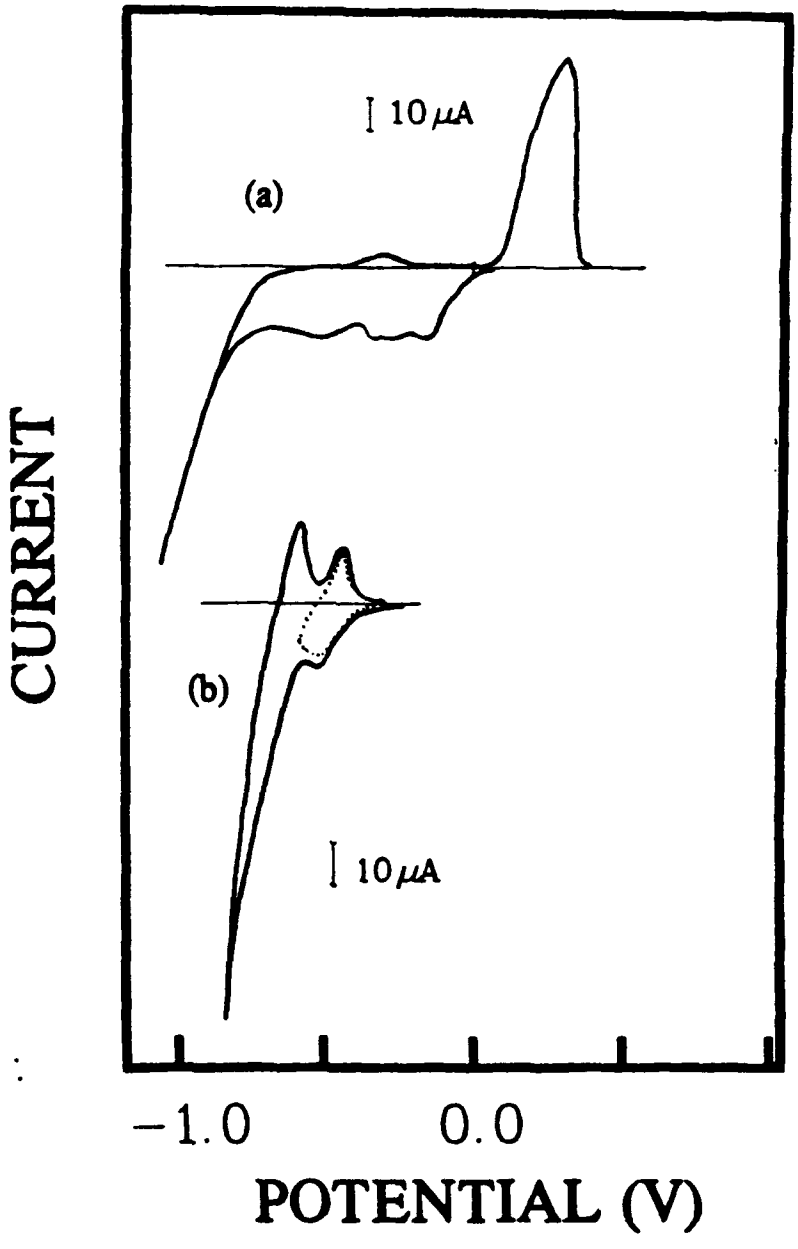


Figure 2. I. Villegas and J.L. Stickney. GaAs Deposition ...

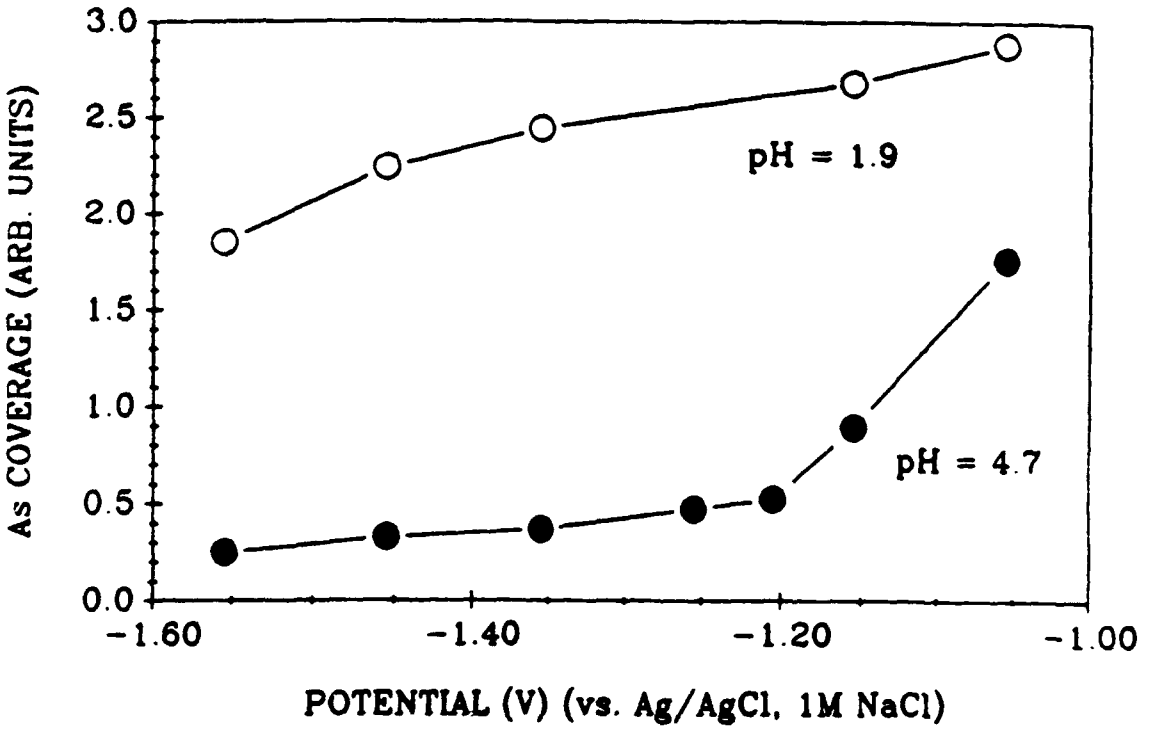


**Figure 3.** I. Villegas and J.L. Stickney. GaAs Deposition ...

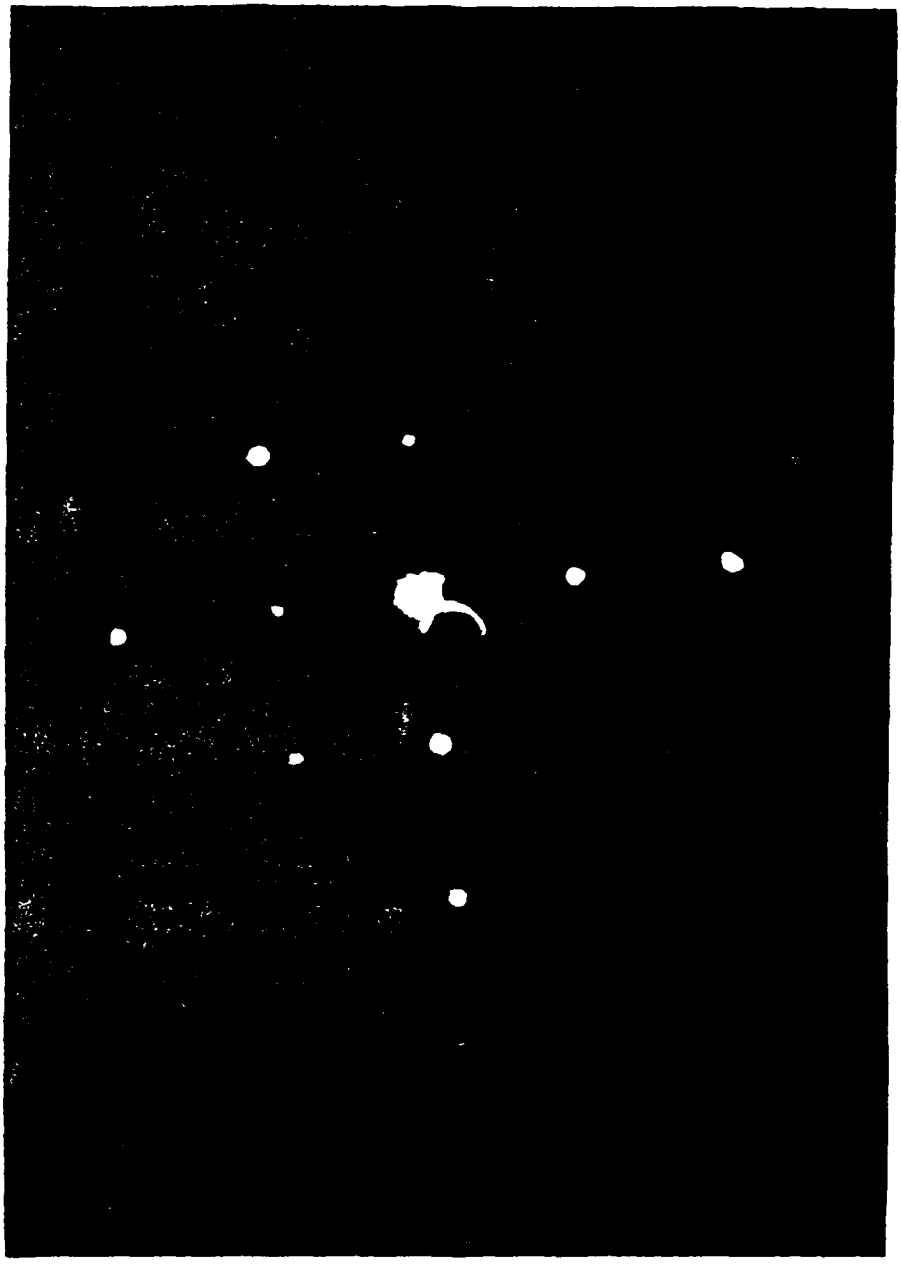

Figure 4a. I. Villegas and J.L. Stickney. GaAs Deposition ...

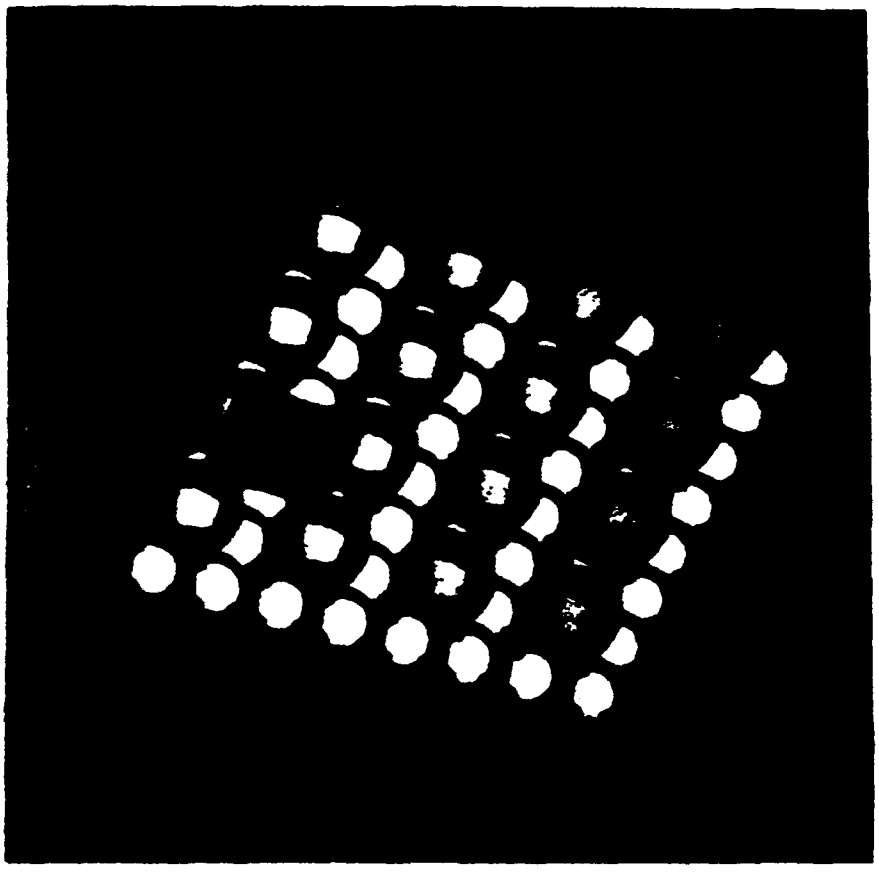

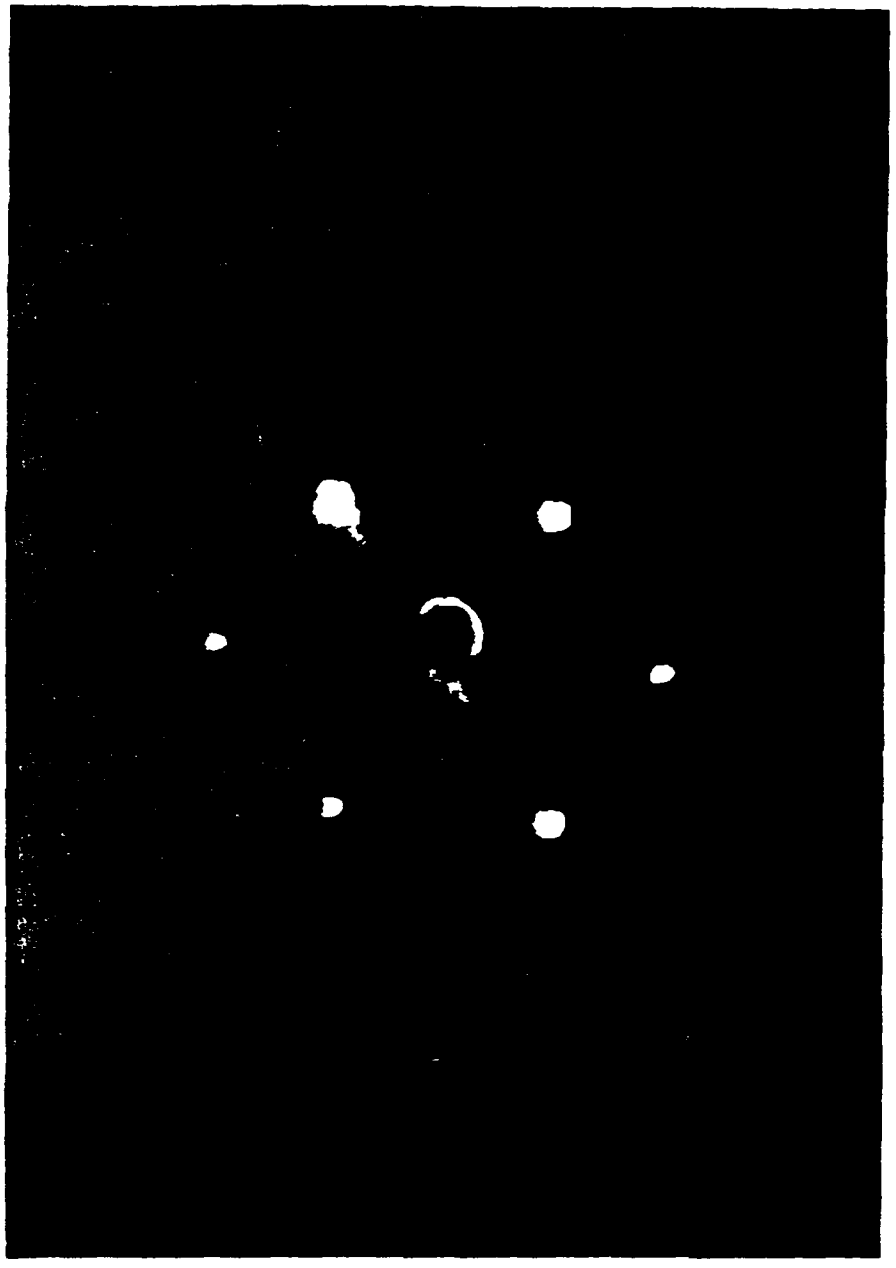

Figure 5a. I. Villegas and J.L. Stickney. GaAs Deposition ...

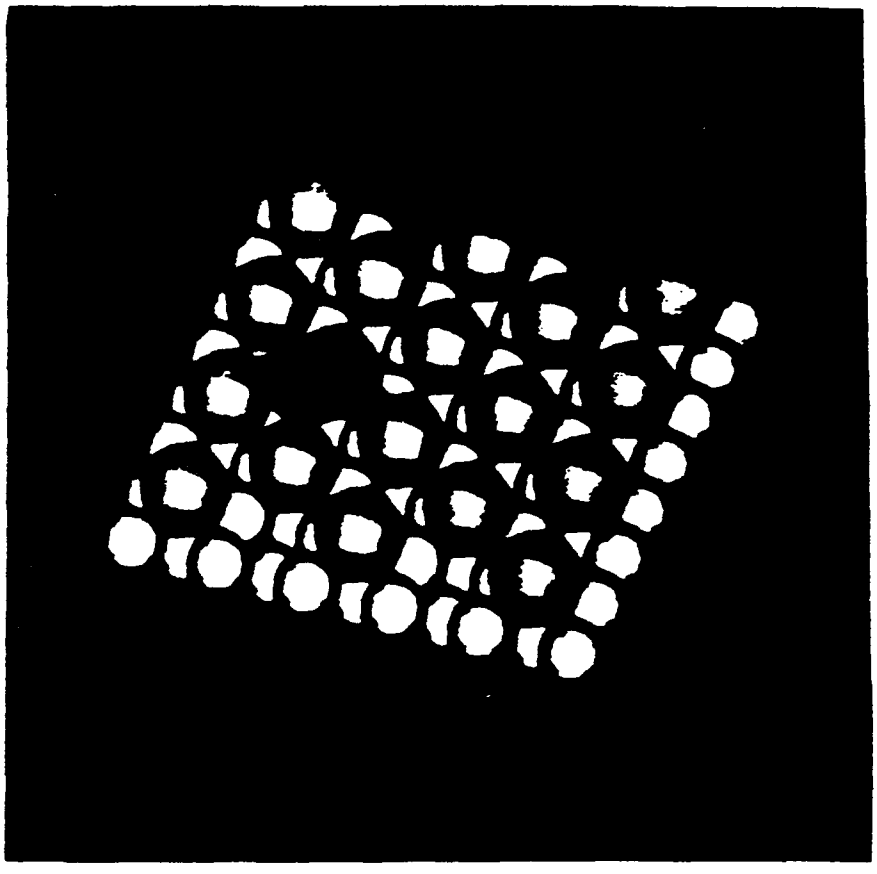

Figure 5b. I. Villegas and J.L. Stickney. GaAs Deposition ...

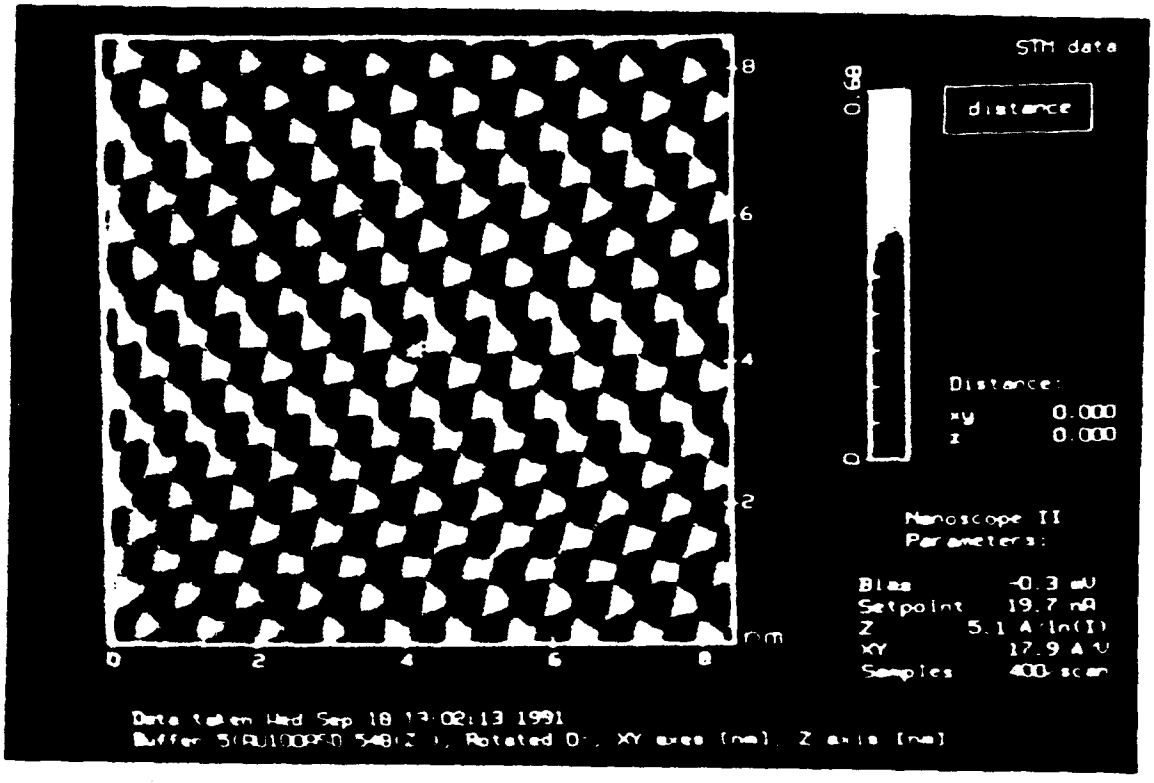


Figure 6. I. Villegas and J.L. Stickney. GaAs Deposition ...

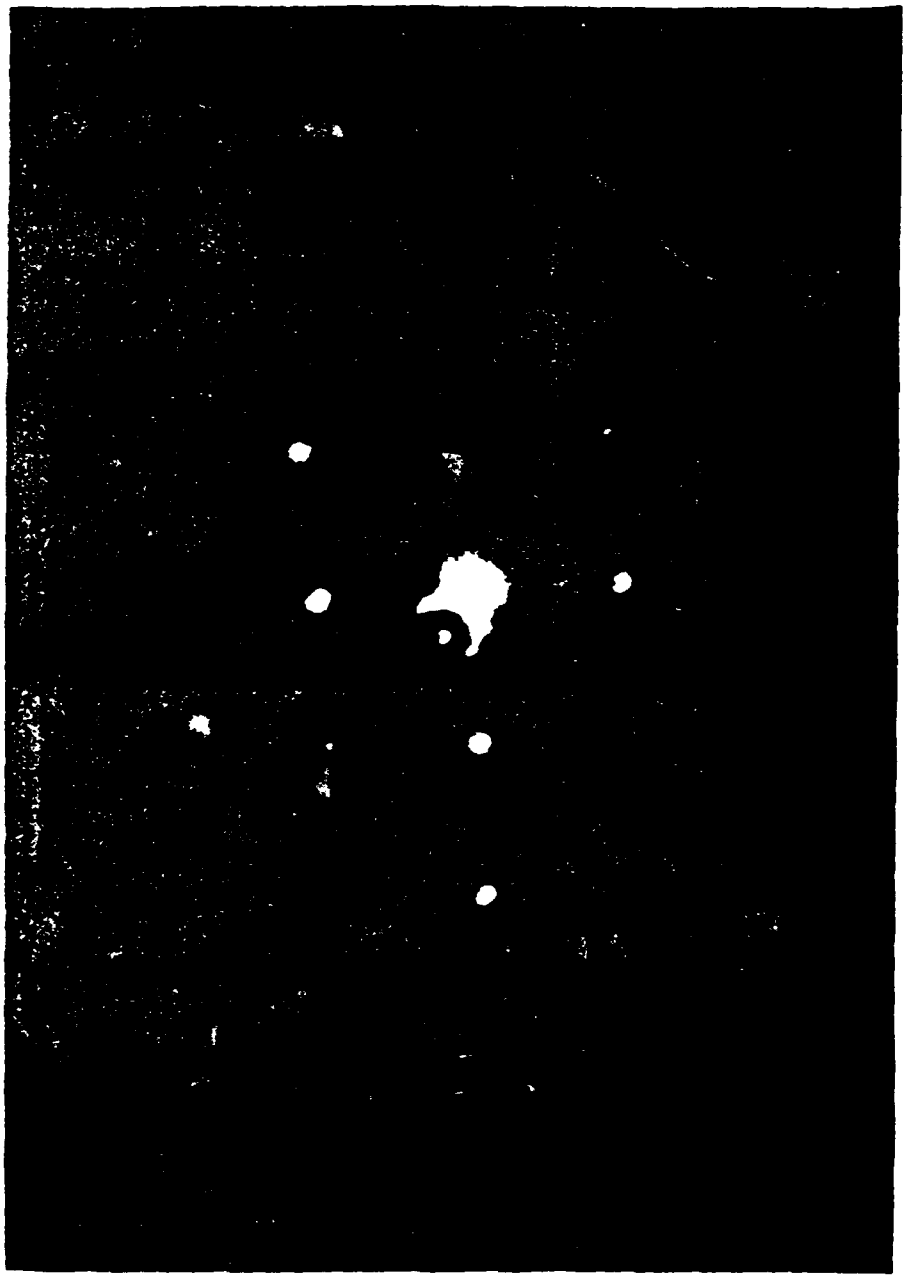

Figure 7a. I. Villegas and J.L. Stickney, GaAs Deposition.

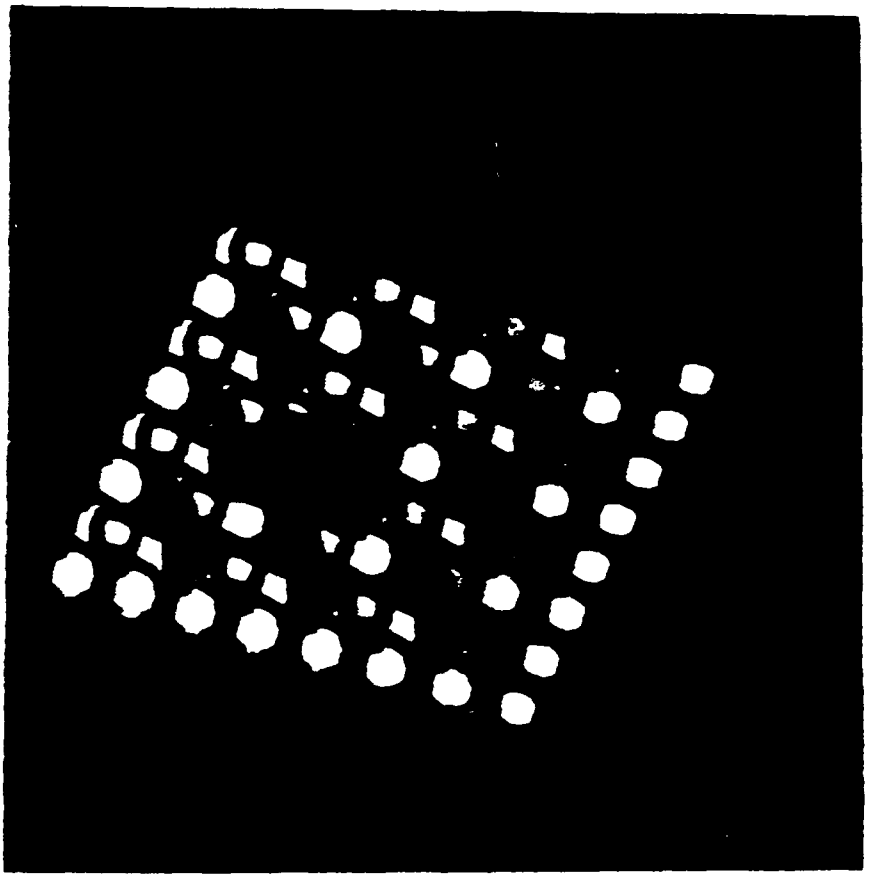

Figure 7b. I. Villegas and J.L. Stickney. GaAs Deposition ...

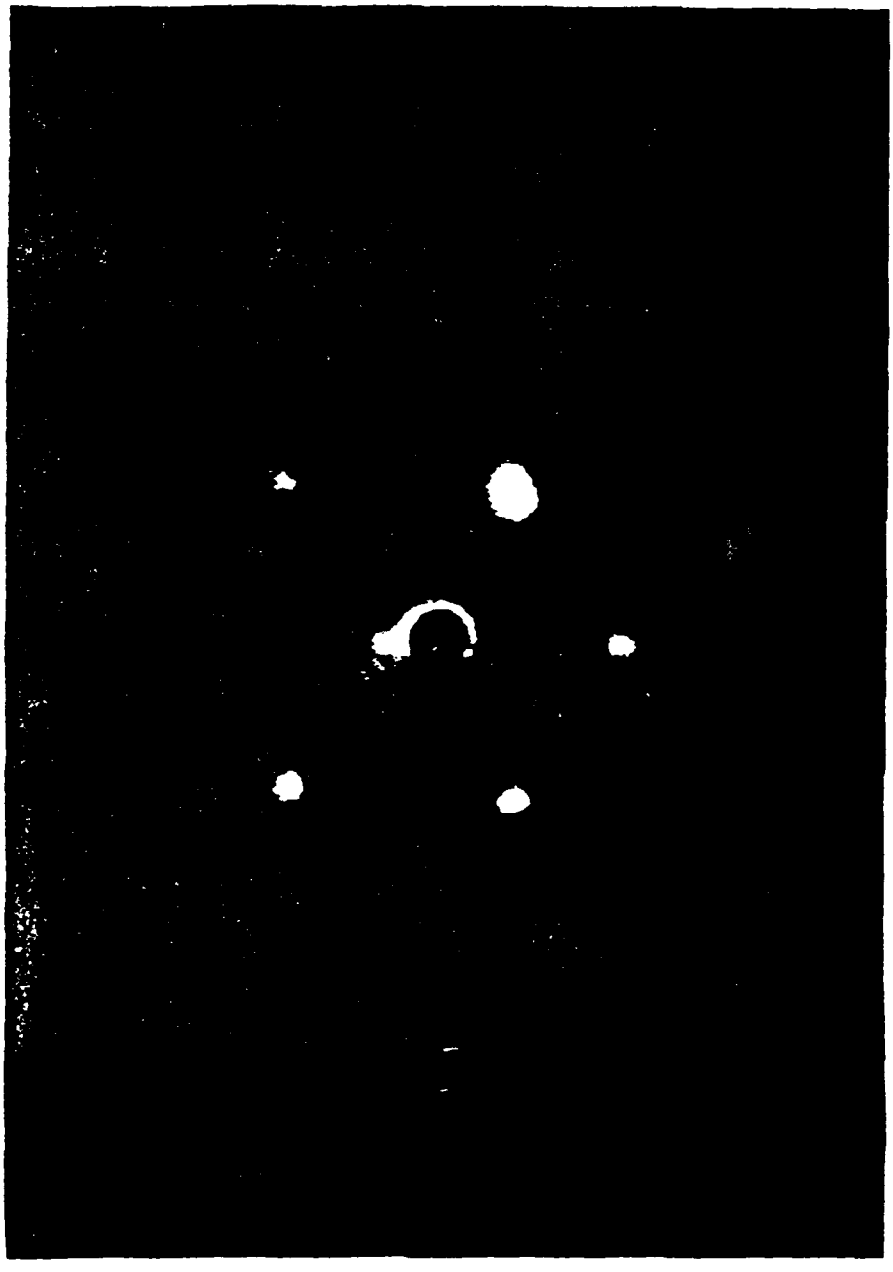

Figure 8a. J. Villegas and J.L. Stickney, GaAs Deposition ...

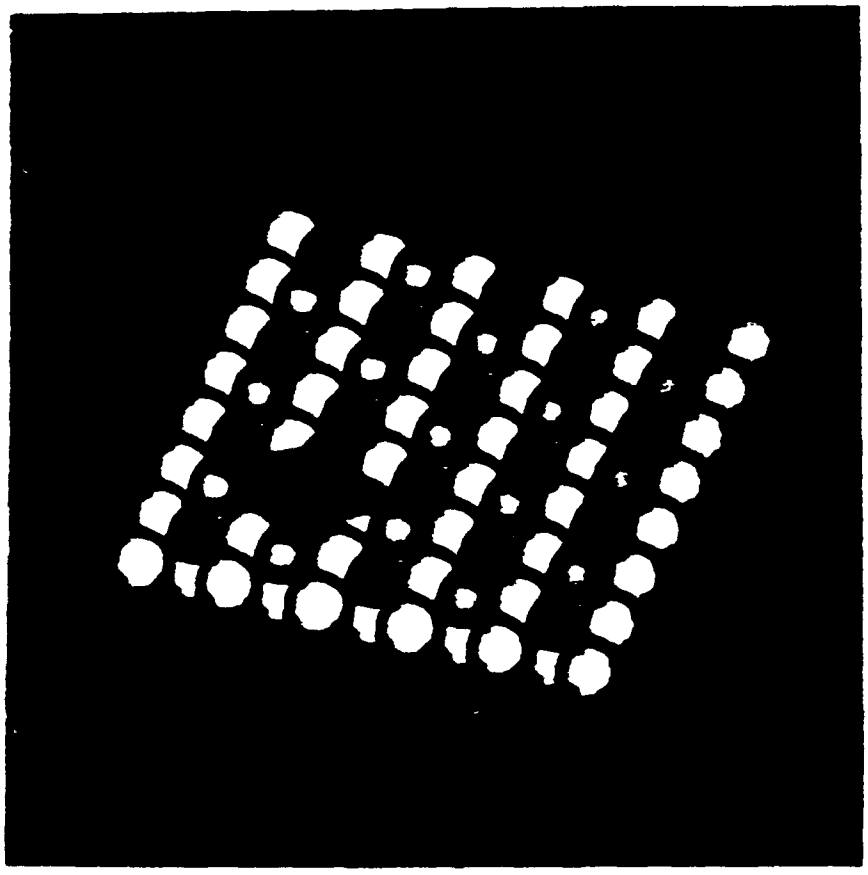

Figure 8b. I. Villegas and J.L. Stickney. GaAs Deposition ...

## TECHNICAL REPORT DISTRIBUTION LIST - GENERAL

Office of Naval Research (2)*
Chemistry Division, Code 1113
800 North Quincy Street
Arlington, Virginia 22217-5000

Dr. James S. Murday (1)
Chemistry Division, Code 6100
Naval Research Laboratory
Washington, D.C. 20375-5000

Dr. Robert Green, Director (1)
Chemistry Division, Code 385
Naval Air Weapons Center
Weapons Division
China Lake, CA 93555-6001

Dr. Elek Lindner (1)
Naval Command, Control and Ocean
Surveillance Center
RDT&E Division
San Diego, CA 92152-5000

Dr. Bernard E. Douda (1)
Crane Division
Naval Surface Warfare Center
Crane, Indiana 47522-5000

Dr. Richard W. Drisko (1)
Naval Civil Engineering
Laboratory
Code L52
Port Hueneme, CA 93043

Dr. Harold H. Singerman (1)
Naval Surface Warfare Center
Carderock Division Detachment
Annapolis, MD 21402-1198

Dr. Eugene C. Fischer (1)
Code 2840
Naval Surface Warfare Center
Carderock Division Detachment
Annapolis, MD 21402-1198

Defense Technical Information
Center (2)
Building 5, Cameron Station
Alexandria, VA 22314

* Number of copies to forward